

# Quokka version 2: selective surface doping, luminescence modeling and data fitting

*Andreas Fell<sup>1\*</sup>, Keith R. McIntosh<sup>2</sup>, Malcolm Abbott<sup>2</sup>, Daniel Walter<sup>1</sup>*

<sup>1</sup> Australian National University, Canberra, Australia

<sup>2</sup> PV Lighthouse, Coledale, Australia

## ABSTRACT

Version 2 of Quokka, a fast and free multidimensional silicon solar cell simulator hosted on [www.pvlighthouse.com.au](http://www.pvlighthouse.com.au) is presented. The primary improvements of version 2 are described, ranging from multiple conductive boundaries, integrated luminescence modeling and optimizer functionality for data fitting purposes. Application examples are given using the optimizer to fit  $J_0_e$  to photo-conductance (PC) measurements in a case where standard methods fail, and fitting local recombination properties to photoluminescence measurements.

## 1. INTRODUCTION

Quokka, the free multi-dimensional solar cell simulator, was recently made available <sup>1</sup>, <sup>2</sup>. It solves the steady state semiconductor carrier transport equations in a simplified manner, utilizing the conductive boundary model and quasi-neutrality condition. In conjunction with an efficient, fully automated meshing algorithm, the simulation speed is orders of magnitude faster than state-of-the art semiconductor device simulators. The settings file generator on the PV Lighthouse website provides a free and user-friendly way of configuring the Quokka simulation. Other available implementations of similar simplified solar cell model are CoBoGUI <sup>3</sup> and PC2D <sup>4</sup>, both are currently restricted to 2D.

Here we describe Quokka's primary new capabilities in version 2, namely multiple conductive boundaries, luminescence modeling and optimizer functionality.

## 2. IMPROVED CAPABILITIES

### 2.1 FRC and IBC version

As with version 1, Quokka 2 features two different cell layouts: front and rear contact (FRC) and interdigitated back contact (IBC), examples are shown in Fig. 1 and Fig. 2 respectively. The FRC layout is more generally applicable, and is suitable for simulating full area rear contact and rear junction cells, as opposed to the previous denotation 'partial rear contact' (PRC).

The terminology of the settings file syntax has been updated to more closely reflect the modeling domain. The boundary definitions are differentiated into conductive and non-conductive boundaries. Conductive boundaries include surface diffusions and other doped surface regions and inversion / accumulation layers characterized by a sheet resistance and majority carrier type. Non-conductive boundaries account for undiffused surfaces. For example, an emitter diffusion is defined as a conductive boundary with a doping type that is opposite to the bulk doping type.

For the FRC version, all conductive boundaries at the front are of opposite type (i.e., emitters), and at the rear are of the

same type, i.e. back surface fields. Rear junction cells can still be modeled by setting the illumination to the rear surface. In the IBC version the emitter is always placed on the left hand side.

## 2.2 Multiple conductive boundaries

In version 2 multiple conductive boundaries with different sheet resistance, shape, dimensions and recombination properties can be defined. One remaining restriction is that each conductive boundary is always centered about the contact of the same polarity. The contact itself has positions that are independently defined. This restriction is consistent with typical cell designs, in particular selective emitter and local BSF cells. Other off-centered conductive boundaries can still be realized by a combination of multiple conductive boundaries with different shapes and dimensions.

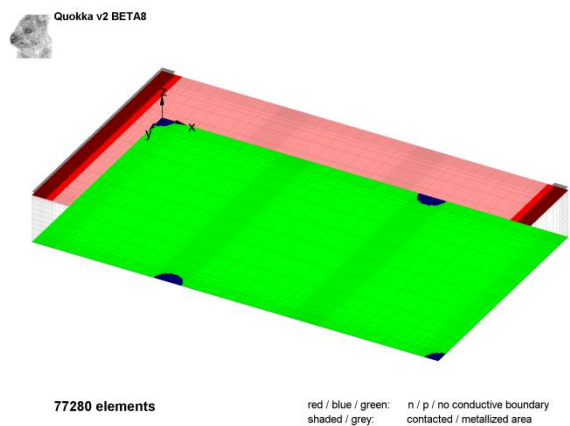


**Fig. 1:** P-type PERL cell with partially contacted selective emitter and local BSF p-type cell with hexagonal rear contact pattern and different front contact / rear contact pitch (1.5 mm / 1 mm); note that the minimal unit cell for front and rear was defined only and Quokka did repeat them to derive the actual common unit cell.

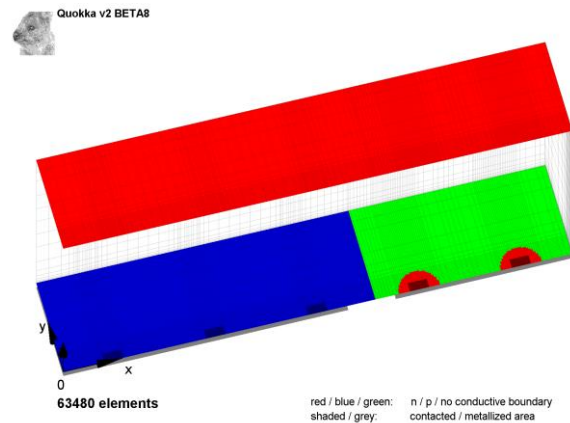


**Fig. 2:** IBC n-type unit cell with locally contacted large area p-type diffusion, partially contacted local n-type diffusion and front floating emitter.

## 2.3 Luminescence modeling

The spectrally resolved silicon emission spectrum has significant diagnostic value, as it is sensitive to lateral and vertical variations in charge carrier distribution. Quokka implements a modular simulation of the luminescence signal by independently simulating the spontaneous emission rate, the photon escape probability, and, if necessary, the efficiency of the detection system. The latter function allows for the inclusion of filtering optics, such as short-pass filters. Quokka's electronic simulation determines the quasi-Fermi energy levels for each unit element, from which the rate of spontaneous emission per energy interval, per solid angle is calculated by the generalized Planck radiation law<sup>5</sup>. By separating the electronic and optical components of the simulation, Quokka can simulate luminescence spectra through low to high (but nondegenerate) injection conditions.

The band-to-band photon emission is subject to reabsorption within the wafer, for which Quokka uses Daub's absorption data as published in<sup>6</sup>. Only a very small percentage of the emission ( $1/4n^2 \approx 2\%$ ) falls within the escape cone, and internally reflected photons are subject to an infinite

series of front and rear reflections. Quokka will produce a hyperspectral luminescence signal map using the escape probability of Schick <sup>7</sup> as a default, applicable for planar surfaces. In the presence of one or more textured surfaces with diffuse reflections, a statistical escape function modeled after Schinke *et al* <sup>6</sup> is implemented, which however doesn't account for the actual spatial smearing and is thus valid for (quasi) 1D simulations only. Figure 3 compares a simulated spectrum for a 1500 $\mu\text{m}$ -thick, semi-planar silicon wafer under monochromatic illumination.

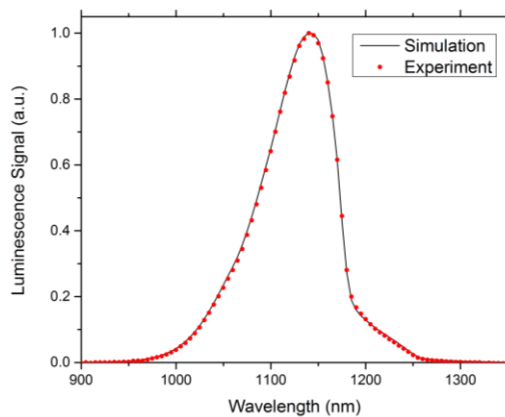


**Fig. 3:** Comparison of simulated and experimentally measured (provided by H. Nguyen) luminescence emission spectrum for a 1500 $\mu\text{m}$  semi-planar silicon wafer under 780nm monochromatic illumination.

## 2.4 Optimizer functionality

With simulation times in the order of seconds even for (simple) 3D cases, Quokka 2 offers the capacity to iteratively fit one or more free parameters to defined goals. The optimizer function essentially uses the Matlab functions 'fgoalattain', which handles arbitrary numbers of fit parameters and goals, or 'lsqnonlin' for least squares curve fitting tasks. The optimizer will accept precise goals such as an effective lifetime, mean PL signal etc., as well as 'min' and 'max' goals, which can be used to maximize cell efficiency for an arbitrary number of free parameters. This flexibility gives

Quokka's fitting capabilities general applicability but care must be taken to define sensible optimization tasks, start values and/or fit parameter bounds. As with any optimization routine, the Quokka optimizer will be susceptible to finding local optima or demonstrate poor convergence behavior in the case of ill-defined optimizations.

For the fit parameters Quokka accepts any scalar simulation input parameters. Goals can be any scalar output values, or, in the case of curve fitting, a vector output produced by one simulation run, e.g. a parameter sweep or light IV-curve. Furthermore, 'overrides' can be defined to account for inter-dependencies between input parameters and fit parameters. The optimizer internally normalizes the parameter and goals by the given (start) values for optimum convergence behavior. Quokka also supports sequential optimization, i.e. performing an identical optimization task multiple times with different input values and / or goal values.

## 3. Application examples

### 3.1 Deriving high $J_{0e}$ from PC measurements

A known limitation of the widely used Kane-Swanson method to derive  $J_{0e}$  from injection dependent effective lifetime measurements is the presence of significant non-uniform carrier distribution within the wafer. This is the case for high  $J_{0e}$  values resulting in an effective minority carrier diffusion length smaller than the wafer thickness, which invalidates the underlying analytical expressions <sup>8</sup>.

Here we show an example of a symmetrically diffused and passivated 345  $\mu\text{m}$  thick 1  $\Omega\text{-cm}$  n-type FZ wafer, which due to some degradation has a high  $J_{0e}$  value. An accurate  $J_{0e}$  value can be

derived by fitting the generalized PC measurement to proper 1D transient simulations, which results in a  $J_{0e}$  of approximately  $1600 \text{ fA/cm}^2$ <sup>9</sup>. Quokka is used for the same purpose, utilizing the optimizer's curve fitting functionality. We define a sweep of suns to generate a  $\tau_{\text{eff}}(\Delta n)$  curve consisting of five points which sufficiently covers the range of interest. The Sinton PC measurement was almost quasi-steady-state, thus we assume a typical Sinton-flash generation profile rather than a uniform one, which would be valid for transient cases. For goal values we import the measured  $\tau_{\text{eff}}(\Delta n)$  curve, define the front  $J_{0e}$  as the fit parameter and override the rear  $J_{0e}$  by the front one to enforce symmetric simulations during the optimization.

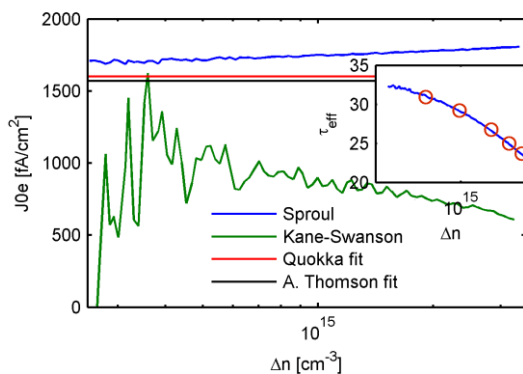


**Fig. 3:** comparison of different methods to derive a high  $J_{0e}$  value; insert shows the optimized Quokka result (red circles) against the measured effective lifetime curve; measurements by A. Thomson<sup>9</sup>;

In Fig. 1 the results of the Kane-Swanson method, the non-simplified original Sproul expressions<sup>10</sup> (converting  $S_{\text{eff}}$  into  $J_{0e}$ ) and the fit results from A. Thomson<sup>9</sup> and Quokka are shown. It is evidenced that analytical approaches are significantly inaccurate in this scenario while both numerical fitting methods give almost identical results. Given the capabilities of the optimizer, this approach can be extended to fit not only a  $J_{0e}$  but e.g. some bulk SRH defect concentration at the same time.

### 3.2 Deriving local recombination properties from PL imaging

For an example on how to derive recombination properties of small local features by PL imaging and Quokka's optimizer, the reader is referred to<sup>11</sup>.

## 4. Conclusions

With version 2, Quokka provides a wider range of capabilities to simulate silicon solar cells. The luminescence modeling and the optimizer functionality can support the characterization of a variety of non-trivial cell and test sample conditions.

## Acknowledgements

The authors acknowledge financial support from the Australian Solar Institute (ASI)/Australian Renewable Energy Agency (ARENA) under the Postdoctoral Fellowship project 5 – F007.

## REFERENCES

- [1] A. Fell, *Electron Devices*, IEEE Transactions on **60** (2), 733-738 (2013).
- [2] [www.pvlighthouse.com.au](http://www.pvlighthouse.com.au), (2013).
- [3] R. Brendel, *Progress in Photovoltaics: Research and Applications* **20** (1), 31-43 (2012).
- [4] P. A. Basore and K. Cabanas-Holmen, *Photovoltaics*, IEEE Journal of **1** (1), 72-77 (2011).
- [5] P. Würfel, S. Finkbeiner and E. Daub, *Applied Physics A* **60** (1), 67-70 (1995).
- [6] C. Schinke, D. Hinken, J. Schmidt, K. Bothe and R. Brendel, *Photovoltaics*, IEEE Journal of **3** (3), 1038-1052 (2013).
- [7] K. Schick, E. Daub, S. Finkbeiner and P. Würfel, *Applied Physics A* **54** (2), 109-114 (1992).
- [8] A. Cuevas, *Solar Energy Materials and Solar Cells* **57** (3), 277-290 (1999).
- [9] A. Thomson, (2013).
- [10] A. B. Sproul, *Journal of Applied Physics* **76** (5), 2851-2854 (1994).
- [11] A. Fell, D. Walter, S. Kluska, E. Franklin and K. Weber, *Energy Procedia* **38** (0), 22-31 (2013)

